





## Article

# Axial Behavior of Concrete-Filled Double-Skin Tubular Stub Columns Incorporating PVC Pipes

Muhammmad Faisal Javed <sup>1,\*</sup>, Haris Rafiq <sup>2</sup>, Mohsin Ali Khan <sup>2,3</sup> , Fahid Aslam <sup>4</sup> ,  
Muhammad Ali Musarat <sup>5,\*</sup>  and Nikolai Ivanovich Vatin <sup>6</sup> 

<sup>1</sup> Department of Civil Engineering, COMSATS University Islamabad, Abbottabad Campus, Abbottabad 22060, Pakistan

<sup>2</sup> Department of Structural Engineering, Military College of Engineering (MCE), National University of Science and Technology (NUST), Islamabad 44000, Pakistan; kh.haris1995@live.com (H.R.); moak.pg18mce@student.nust.edu.pk (M.A.K.)

<sup>3</sup> Department of Civil Engineering, CECOS University of IT and Emerging Sciences, Peshawar 25000, Pakistan

<sup>4</sup> Department of Civil Engineering, College of Engineering in Al-Kharj, Prince Sattam Bin Abdulaziz University, Al-Kharj 11942, Saudi Arabia; f.aslam@psau.edu.sa

<sup>5</sup> Department of Civil and Environmental Engineering, University Teknologi PETRONAS, Bandar Seri Iskandar 32610, Malaysia

<sup>6</sup> Peter the Great St. Petersburg Polytechnic University, 195291 St. Petersburg, Russia; vatin@mail.ru

\* Correspondence: arbab\_faisal@yahoo.com (M.F.J.); muhammad\_19000316@utp.edu.my (M.A.M.)

**Abstract:** This experimental study presents concrete-filled double-skin tubular columns and demonstrates their expected advantages. These columns consist of an outer steel tube, an inner steel tube, and concrete sandwiched between two tubes. The influence of the outer-to-inner tube dimension ratio, outer tube to thickness ratio, and type of inner tube material (steel, PVC pipe) on the ultimate axial capacity of concrete-filled double-skin tubular columns is studied. It is found that the yield strength of the inner tube does not significantly affect the ultimate axial capacity of concrete-filled double-skin tubular composites. With the replacement of the inner tube of steel with a PVC pipe, on average, less than 10% strength is reduced, irrespective of size and dimensions of the steel tube. Hence, the cost of a project can be reduced by replacing inner steel tubes with a PVC pipes. Finally, the experimental results are compared with the existing design methods presented in AISC 360-16 (2016), GB51367 (2019), and EC4 (2004). It is found from the comparison that GB51367 (2019) gives better results, followed by AISC (2016) and EC4 (2004).

**Keywords:** concrete-filled double-skin tubular columns; PVC pipes; steel tubes; axial capacity; stub columns; multiphysics model



**Citation:** Javed, M.F.; Rafiq, H.; Khan, M.A.; Aslam, F.; Musarat, M.A.; Vatin, N.I. Axial Behavior of Concrete-Filled Double-Skin Tubular Stub Columns Incorporating PVC Pipes. *Crystals* **2021**, *11*, 1434. <https://doi.org/10.3390/cryst11121434>

Academic Editors: José L. García and Chongchong Qi

Received: 22 October 2021

Accepted: 16 November 2021

Published: 23 November 2021

**Publisher's Note:** MDPI stays neutral with regard to jurisdictional claims in published maps and institutional affiliations.



**Copyright:** © 2021 by the authors. Licensee MDPI, Basel, Switzerland. This article is an open access article distributed under the terms and conditions of the Creative Commons Attribution (CC BY) license (<https://creativecommons.org/licenses/by/4.0/>).

## 1. Introduction

Conventional reinforced concrete has been largely used to construct composite structures [1,2]. With a growing demand for high-rise structures, it is difficult and impossible to use reinforced concrete due to its low strength-to-weight ratio [3]. While, on the other hand, an exponential rise in the use of steel structures has been observed [4]. This increase is due to steel properties resistant to both compressive and tensile loading [5]. The advancement in technology has developed new methods of constructing engineering structures. Engineers widely use concrete-filled steel tubes (CFSTs) in high-rise buildings due to their numerous advantages in normal and extreme weather conditions [6–17]. Different variants of CFSTs have also been employed due to their better performance. A recycled aggregate infilled CFST [13], preplaced aggregate CFST [14], multi-cell composite CFST [16], CFST with external steel confinement [18], and concrete-filled double steel tubes (CFDSTs) [19,20] are some of the common types of CFSTs currently being used. CFDST columns are composite columns with outer and inner steel tubes, whereas concrete is sandwiched between these tubes. Different types of CFDSTs and CFSTs are shown in Figure 1. CFDST columns

have found many practical applications in the construction industry due to their unending advantages [21]. These columns do not need formwork for their construction as outer and inner steel sections act as a case to perform this function [22]. The absence of formwork can lead to faster construction, which can significantly reduce the project's cost [23]. The CFDST columns are lighter in weight as concrete in a core is replaced by the inner hollow steel section [23]. The CFDST columns have increased strength due to the confinement of concrete provided by inner and outer steel sections, and these columns show good resistance to wind and earthquake loading by dumping their vibrations [24–26]. Besides that, CFDSTs with a greater internal hollow area can be utilized as submarine pipelines, offshore platform legs, subsurface embedded pipeline cabins and corridors, etc. [27], since they have a greater stiffness and axial capacity, and a longer lifespan than conventional reinforced concrete.

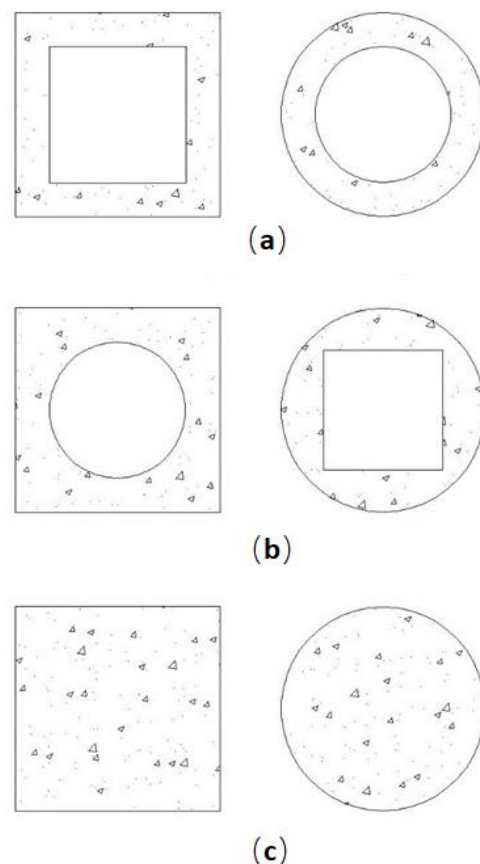


**Figure 1.** Different typologies of CFDSTs and CFSTs (a) CFDST with similar sections (b) CFDST with different sections (c) CFST with SHS and CHS.

The structural behavior of CFDST columns has been studied by numerous authors, both experimentally and numerically. Most of the tests were performed on circular CFSTs, and later on square and rectangular-shaped tubes. Furthermore, in most studies, the shape of the outer and inner steel tubes has been the same. Zhao and Grzebieta [28] performed experimental tests on square–square CFDST columns, subjected only to an axial load, filled with normal strength concrete, and studied the ductility and plasticity of CFDST columns. Uenaka et al. [25] studied the axial behavior of thin-walled circular–circular CFDST columns. They concluded that the inner tube did not utilize its full strength due to the buckling of the outer steel tube. Tao et al. [29] studied CFDST columns subjected to eccentric loads. The analytical method was proposed based on the vast experimental tests conducted on circular–circular CFDSTs. It was concluded that circular–circular CFDST columns fail in global buckling when subjected to an eccentric load. Tests on

rectangular–rectangular CFDST beam-columns were reported by [30]. Li et al. [31,32] performed experimental tests on CFDST columns with an inner and outer tube of a circular geometrical shape, while Han et al. [33] reported tests on elliptically shaped CFDST columns with a variation in the type of steel used in the outer and inner sections. Moreover, Han et al. [34] also proposed a novel non-linear concrete modelling approach to examine CFDST columns and validate them through a comparison with the experimental tests findings of other scholars.

Additionally, the research findings explain that the CFDST column has a much greater strength than the summation of strengths of an inner tube, outer tube, and compressive strength of concrete, separately [35]. Dong and Ho [36] empirically examined the performance of CFDST columns with respect to stiffness and strength having externally bonded steel rings under a compression load. The comparison of their findings, with CFDST columns lacking outside confinement, reveals that using external steel rings for the confinement of CFDST columns greatly improved their load-carrying capacity, ductility, and stiffness. Haas and Koen [37] used two distinct lengths and hollowness ratios and investigated the performance of CFDST columns with eccentric loading. They discovered that the axial capacity decreased with the increase in the length and hollowness ratio. Romero et al. [38] reported the experimental response of six circular CFDST slender columns infilled with high strength and normal strength concrete under elevated and ambient temperatures. They found that the buckling load (i.e., 1644 kN) was the same for ambient and elevated temperatures, regardless of the location of the slightly thicker tube (inner or outer). They also found that the layout of the examined specimens had a substantial impact on their fire-resistant performance.

CFDST columns with different inner and outer steel tubes have also been studied by a few researchers [39,40]. Elchalakani et al. [40] studied short circular–square CFDSTs filled with high-strength concrete. The author compared the results with three different design codes using a multiphysics model. Tests on square–circular columns were reported by Han et al. [39]. Yang et al. [41] performed experimental tests on a different combination of outer and inner steel tube shapes. They concluded that circular columns performed better, followed by outer-square inner-circular sections. However, studies have shown that a circular hollow section (CHS), used as an outer tube, provides good confinement to concrete. In contrast, a square hollow section (SHS) is easier to fabricate and install a beam-to-column connection [41]. Hence, CFDST columns with a CHS on the interior side and a square hollow section (SHS) on the exterior side is used in this research.

As in CFDST columns, the primary objective of the inner tube is to provide formwork (although, in some cases, it resists some external compressive forces); it is economical to provide a thinner inner tube than the outer tube. However, the thinner tubes are vulnerable to buckling. As an alternative, the use of other materials would be a smart choice. This paper proposed a kind of composite column, namely, concrete-filled circular steel tubular columns with an inner circular PVC pipe, “CFSPT column”. By replacing the internal steel tube of CFDST columns with a circular PVC pipe, low-cost and eco-friendly CFSPT columns can be prepared with enhanced properties. The advantages of combining the three kinds of materials are expected to be the sandwiched concrete being better confined by the PVC pipe and the steel tube, the sandwiched concrete being able to delay the local buckling of the steel tube, and the buckling of the inner slender PVC column and the splitting of the PVC pipe also being restrained. Thus, compared with the CFDST column, the better ductility of the CFSPT column can be achieved. As for its connection system, CFDST columns to steel beam connections using diaphragms or blinded bolts can be adopted [42]. Detailed experimental work is reported in this manuscript to study, in detail, the axial behavior of CFSPT columns. The inner steel tube is replaced with a PVC pipe to decrease the overall cost of the member. The effect of the slenderness of the outer tube and outer-to-inner tube dimensions ratio is also studied. The performance of concrete-filled steel plastic tubes (CFSPT) is compared with the CFDST performance. Finally, the experimental

results of the multiphysics model are compared with the available design codes to check the applicability of existing codes on the CFSPT.

## 2. Materials and Methods

### 2.1. Specimen Preparation

The CFDST columns investigated consisted of an outer square steel tube, a circular inner tube, and concrete in between the two tubes. A total of 24 specimens were cast for this experimental study. Figure 2 shows the geometry and terminology of the composite column used in this research. In Figure 2,  $B_o$  represents the outer width of the composite column,  $D_i$  shows the diameter of the inner steel tube,  $t_o$  shows the thickness of the steel tube, and  $t_i$  is the thickness of plastic tube. The details of the casted specimens are shown in Table 1. The number of specimens was chosen based on the parameters to be studied. All the specimens were tested at 28 days.

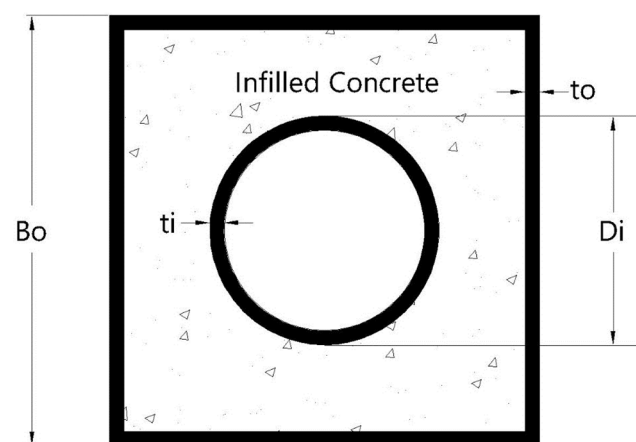


Figure 2. Geometry of specimen with outer SHS and inner CHS.

Table 1. Specimen designation and their dimensions.

Specimen Name	Group of Combinations	Outer Width (mm)	Inner Diameter (mm)	Type of Inner Tube	Bo/Di Ratio	Bo/to Ratio
SS100-37.5	G1	100	37.5	Steel	2.67	83.30
SS100-31.25		100	31.25	Steel	3.20	83.30
SS75-37.5		75	37.5	Steel	2.00	62.40
SS75-31.25		75	31.25	Steel	2.40	62.40
SP100-37.5	G2	100	37.5	Plastic	2.67	83.30
SP100-31.25		100	31.25	Plastic	3.20	83.30
SP75-37.5		75	37.5	Plastic	2.00	62.40
SP75-31.25		75	31.25	Plastic	2.40	62.40

Table 1 shows eight different combinations used in the research. The combinations were divided into two broad groups based on the type of inner tube. Three samples were cast, for each combination, to enhance the accuracy of the results. “G1” and “G2” groups contained CFDST and CFSPT columns, respectively. ( $B_o/D_i$ ) varied from 2 to 3.2 in a group. The rest of the dimensions of CFDST columns were kept constant in both groups. For instance, the SS100-37.5 represents a concrete-filled double-skin tube constructed with inner and outer steel tubes with 37.5 mm and 100 mm in diameter, respectively, while SP75-31.25 represents concrete-filled double-skin tube constructed with inner plastic tube and outer steel tube having width 31.25 mm and diameter 75 mm, respectively. Using the various combinations of casted samples tabulated in Table 1, the effect of the inner tube on the ultimate axial capacity of CFDST and CFSPT columns was studied.

## 2.2. Properties of Concrete

The ACI mix design procedure was followed to prepare a concrete mix with proportions of 1:1.5:3 (representing parts of cement, fine aggregate, and coarse aggregate, respectively), i.e., M20 concrete, to achieve the design strength of 20 MPa. The study was based in Pakistan, where concrete is usually produced with 20 MPa of targeted compressive strength [43]. A water–cement ratio of 0.55 was considered in this research to attain the higher workability of concrete. Water absorption for both coarse and fine aggregates was measured to be 1%. Ordinary Portland cement with a specific gravity of 3.1 was used in this research. Specific gravities for fine and coarse aggregate were 2.65 and 2.6, respectively. Coarse aggregates had a nominal maximum size of 20 mm, while fine aggregates with a size less than 4.75 mm were considered. Six cylinders and three cubes were cast (with the same proportions) to determine the stress–strain curve and strength of infilled concrete to be used in columns. The stress–strain graph of the used concrete is provided in Figure 3. Ingredients were mixed, cast, and cured according to the ASTM standard [44]. Concrete was placed in three layers and was properly compacted with a mechanical vibrator. As the specimens did not need any formwork, the specimens were covered with plastic bags from the top immediately after casting.

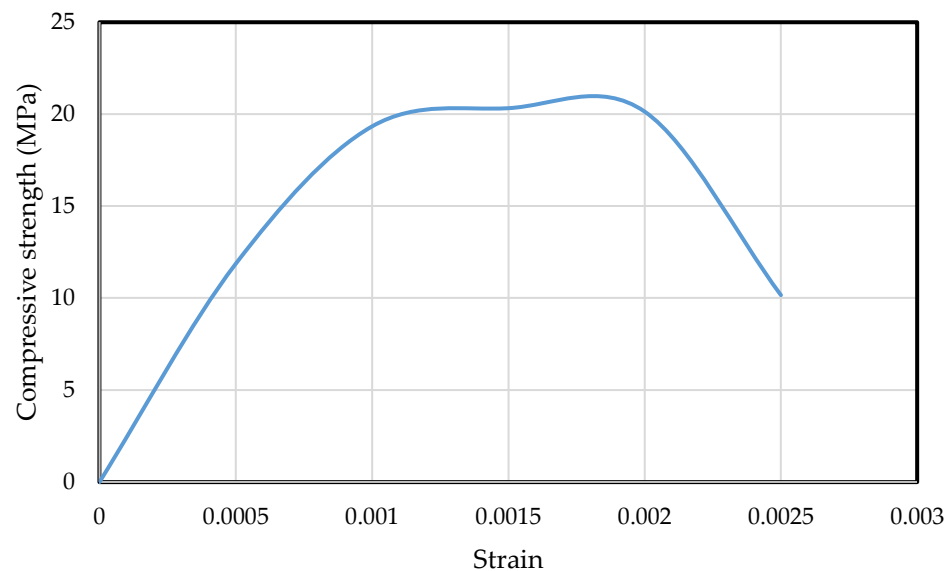


**Figure 3.** Stress–strain graph of the concrete used in this research.

## 2.3. Properties of Steel Tubes

The steel used in this research was cold-formed mild steel with an average amount of carbon content varying between 0.05% and 0.25% by weight. Two different dimensions of SHS, CHS, and PVC pipe were selected to serve the purpose of confinement tubes as described earlier. A flat steel plate was used as a base plate to construct CFDST columns. The top of the plate was marked to ensure that the inner tube was placed right in the center of the outer tube. Tensile tests were performed on the rolls from which square and circular sections were created according to the ASTM standard [45]. Specifically, ASTM D876 was used for finding out the tensile strength of the PVC tubes. Table 2 shows the yield strength for all the samples. It must be noted that there was a difference between yield strengths of square and circular X-sections.

**Table 2.** Properties of materials.

Tube Type	Yield Strength (MPa)	Ultimate Strength (MPa)	Elastic Modulus (MPa)	Poisson's Ratio
Square steel	210	350	210,000	0.3
Circular steel	300	362	205,000	0.3
PVC	50	70	2620	0.34
Concrete	18	20	35,300	0.2

Furthermore, the yield strength was different even for the same cross-section. This difference was kept intentionally to study the effect of the yield strength of steel on the behavior of samples. The length or height of all the samples used for every test conducted was kept as 150 mm.

#### 2.4. Properties of PVC Pipes

Circular PVC pipes were obtained from Alpha Pipe Industries Abbottabad, Pakistan, and used to replace inner steel tubes in 12 samples. The diameter and thickness of PVC pipes were kept the same as steel tubes for easy comparison. However, the yield strength of PVC pipes was calculated using tensile test machine (ASTM D876) performed in the laboratory and is shown in Table 2.

#### 2.5. Test Procedure

After 28 days of curing, prepared specimens were tested in a hydraulic compression testing machine with a maximum capacity of 2000 KN. Displacement-controlled load was applied, as suggested in available literature [46,47], at the top end of the specimen with the help of a thick steel plate that distributed the load uniformly. The digital meter recorded the peak load when the specimen failed. All tests were conducted in the concrete testing laboratory of COMSATS University, Abbottabad Campus.

### 3. Results and Discussion

The axial compressive strength and failure modes of all the columns were presented in this section to discuss the influence of different parameters on the axial behavior of CFDSTs and CFDPTs. The parameters included the slenderness of the outer tube, the type of material of the inner tube, and  $B_o/D_i$ . Furthermore, a comparison of the performance of CFDST columns against CFSPT columns revealed the contribution of the inner tubes on the strength index and concrete contribution ratio.

#### 3.1. Failure Modes

Figure 4 shows the failure modes of CFDST and CFSPT tubes. All columns failed due to the local failure of tubes and the yielding of steel. The local failure of steel tubes was more prominent in larger sections as compared to smaller sections. In concrete, shear failure was observed after the crushing mode. Furthermore, it was noted that the type of material (pipe or steel) did not prevent the shear failure of concrete. After testing, all the specimens were cut in the middle, and a smooth inner surface of the shell concrete was observed, showing a proper compaction. Similar observations were reported in the literature for stainless CFDSTs [48,49].



**Figure 4.** The failure mode of all tested specimens.

### 3.2. Effect of Inner Tube of Distinct Materials

The use of composite construction (i.e., CFDSTs) is increasing with time. Different ways were used to analyze the performance of composite columns as composite construction is considered strong in terms of its load-carrying performance regardless of its construction cost. The use of a PVC tube as an inner tube in a concrete-filled double-skin tube can lead to the lower construction cost. Thus, it is necessary to analyze the performance equivalency of CFDSTs and CFPSTs. Figure 5 shows the comparison between the axial capacities of CFDSTs and CFPSTs. It was observed that by replacing the inner tube of steel with a PVC pipe, on average, less than 10% strength was reduced irrespective of size and dimensions of the steel tube. This reduction may be due to a lesser contribution of the inner tube to the ultimate axial capacity of the CFDST and CFPST columns. The inner tube did not perform to its maximum capacity as the outer tube underwent buckling before yielding the inner tube. Various researchers concluded similar results for long CFDSTs and stainless CFDSTs. Hence, it can be concluded that the performance of CFPSTs was almost equal to CFDSTs, despite the reduced cost of the PVC pipe. Thus, CFPSTs can be used as an effective practical alternative to CFDSTs.

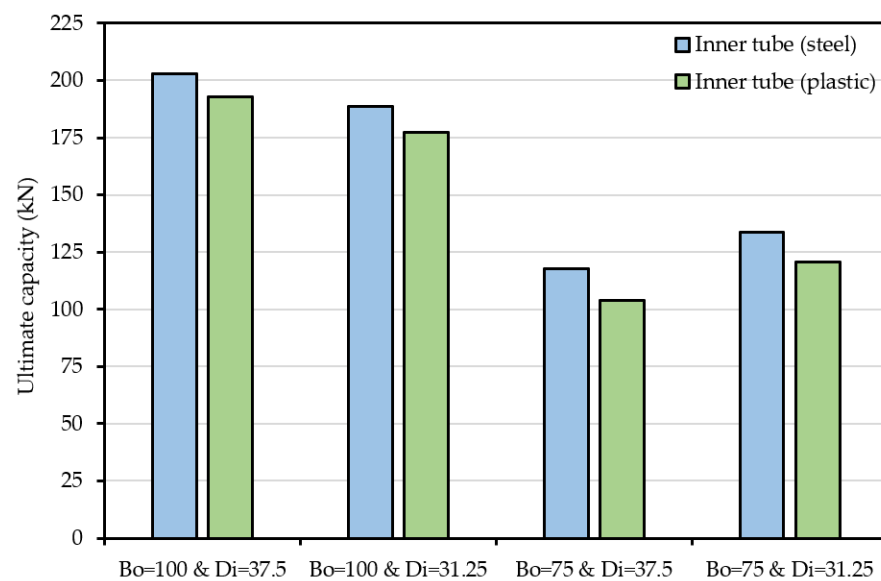


Figure 5. Strength comparison between CFDST and CFSPT columns.

### 3.3. Effect of Bo/t Outer Tube Slenderness

Eight different sets of CFDST and CFSPT samples (three for each set) were tested with varying Bo/t. The overall experimental results of these samples, along with the code comparison, are shown in Tables 3 and 4. The average strength of CFDSTs (1st and 3rd sample) was reduced by 42% (from 202 to 117) when the Bo/t of the outer tube was reduced by 25% (from 83.33 to 62.5). A similar reduction in the axial capacity of CFSPTs was observed for similar changes in the slenderness of the outer tube. The strength reduction due to a reduced Bo/t was less for the smaller diameter of inner tube for both CFSPTs and CFDSTs as shown in Figure 6. However, for a similar reduction in Bo/t, the strength of CFSPTs was reduced by 47% (from 192 to 103). The difference in strength reduction was not significant and showed the superiority of CFSPTs, as PVC pipes are much cheaper than steel. Similar conclusions were reported in the literature and were due to failure to utilize the full capacity of inner tubes in the case of the low slenderness of the outer tube [50,51].

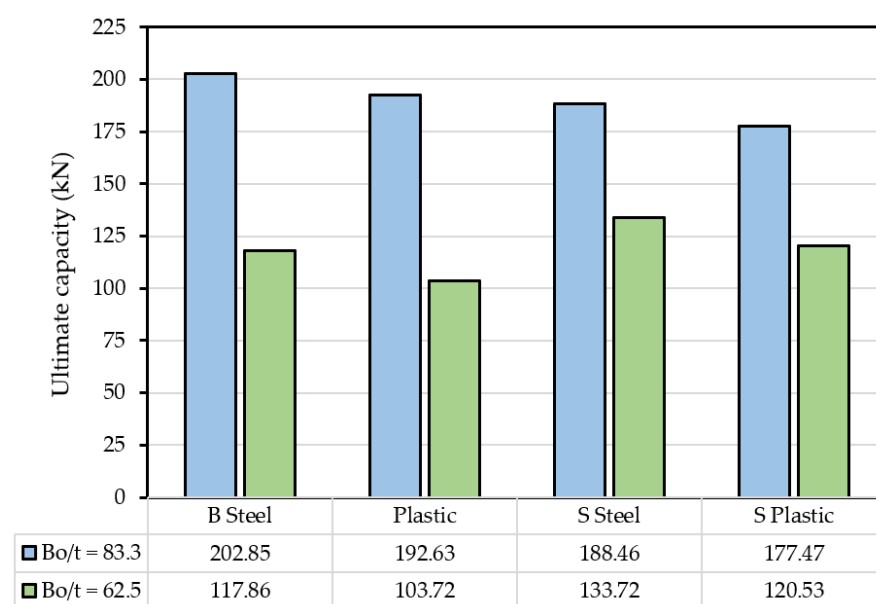


Figure 6. Comparison of axial capacities for different Bo/t ratios.



### 3.4. Effect of Outer-to-Inner Tube Dimension Ratio

Figure 7 compares the ultimate axial compression values to show the effect of the Bo/Di tube ratio. Four different Bo/Di ratios were used in this study for CFDSTs and CFSPTs. The effect of changing Bo/Di was the same on CFDSTs and CFSPTs. Furthermore, increasing the Bo/Di ratio from 2 to 2.67 resulted in a higher ultimate capacity. This higher ultimate capacity was due to the higher effect of confinement, more contact area, and higher amount of steel [52]. However, upon further increasing Bo/Di, the ultimate capacity decreased. The decrease may have been the result of the poor compaction of infilled concrete [53].

Furthermore, it may be due to steel buckling as the advantage of concrete was not fully utilized due to a lesser amount of concrete. Hence, it can be concluded that the careful selection of Bo/Di must be taken into consideration to fully utilize the advantages of CFDSTs and CFSPTs. Furthermore, the optimum Bo/Di ratio was the same for CFDSTs and CFSPTs, showing a similar behavior of both columns.

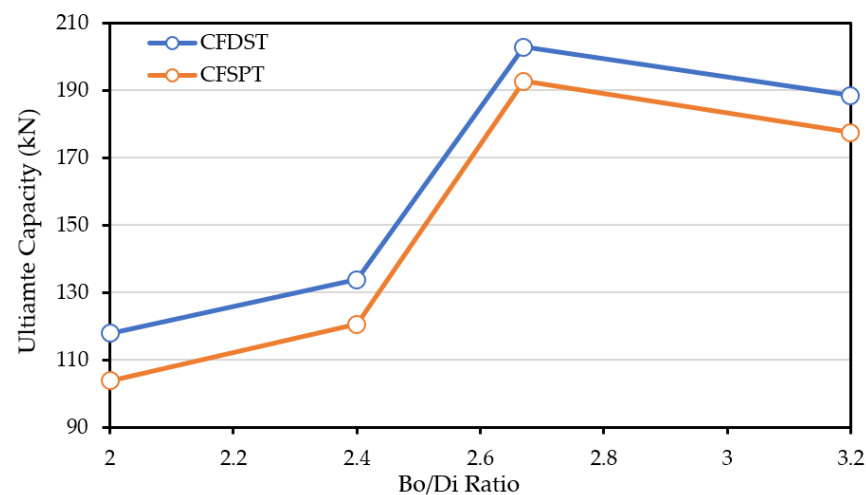


**Figure 7.** Comparison of CFDST and CFSPT columns at varying inner-to-outer tube ratios.

### 3.5. Effect of Inner Tube on Strength Index

Numerous researchers used a strength index to compare the ultimate axial capacities of CFDST columns with the theoretical estimated ultimate capacities [33,54–56]. The strength index was calculated using Equation (1):

$$\text{Strength index} = SI = \frac{P(EXP)}{A_{os}.f_{yo} + A_{is}.f_{yi} + A_c.f'_c} \quad (1)$$

where  $A_{os}$ ,  $A_{is}$ , and  $A_c$  are the cross-sectional areas of the outer tube, inner tube, and infilled concrete, respectively. Table 3 presents the comparison of the Strength Index (SI) on the strength of CFDSTs and CFSPTs. It can be observed that the value of SI was largely lesser than the unity for CFDST and CFSPT columns, which meant a simple arithmetic sum of individual strengths over predicted the capacity of slender CFDST columns. Furthermore, SI did not vary largely regardless of the inner tube of distinct materials.

**Table 3.** SI and CCR of all the tested specimens.

Specimen Name	$A_{os}$ (mm <sup>2</sup> )	$A_{is}$ (mm <sup>2</sup> )	$A_c$ (mm <sup>2</sup> )	SI	CCR
SS100-37.5	480	141.37	8657.5	0.69	1.41
SS100-31.25	480	117.81	8994.8	0.64	1.38
SS75-37.5	360	141.37	4342.5	0.58	0.93
SS75-31.25	360	117.81	4679.8	0.67	1.13
SP100-37.5	480	141.37	8657.5	0.75	1.78
SP100-31.25	480	117.81	8994.8	0.68	1.67
SP75-37.5	360	141.37	4342.5	0.63	1.15
SP75-31.25	360	117.81	4679.8	0.71	1.36

**Table 4.** Ultimate capacity obtained from experimental tests and different design codes.

Specimen Name	$B_0/D_i$	Average $P_{Exp}$ (kN)	$P_{AISC}$ (kN)	$P_{HAN}$ (kN)	$P_{EC4}$ (kN)
SS100-37.5	2.67	202.85	251	254	269
SS100-31.25	3.20	188.46	250	249	269
SS75-37.5	2.00	117.86	164	182	167
SS75-31.25	2.40	133.72	162	177	167
SP100-37.5	2.67	192.63	220	197	239
SP100-31.25	3.20	177.47	224	202	243
SP75-37.5	2.00	103.72	135	126	141
SP75-31.25	2.40	120.53	139	130	145

### 3.6. Effect of Inner Tube on Concrete Contribution Ratio

The concrete contribution ratio (CCR) was calculated using Equation (2) to compare the contribution of infilled concrete to the ultimate axial capacity of CFDST and CFSPT columns:

$$CCR = \frac{P(EXP)}{A_{os}.f_{yo} + A_{is}.f_{yi}} \quad (2)$$

where  $A_{os}$  and  $A_{is}$  are the cross-sectional areas of the outer and inner tubes, respectively. Table 3 presents the comparison between CFDSTs and CFSPTs based on the CCR. It was observed that the CCR did not vary largely, regardless of the inner tube of distinct materials. The average value of CCR in the case of CFSPT was 27.5% greater than CFDST. Thus, it can be concluded that PVC pipe as an inner tube did not largely affect the CCR of infilled concrete.

### 3.7. Axial Capacity of CFDST Column

Experimental results of CFDST specimens were compared with the compressive strength obtained using design equations of AISC 360-16 (2016), GB51367 (2019), and EC4 (2004). In most of the cases, these codes gave conservative results due to the consideration of several basic assumptions, which were not applicable in composite construction. All the specimens studied in this research had an outer section slenderness in the category of very slender as specified in EC4.

#### 3.7.1. AISC Specifications

The AISC equation derivation worked on the same concept as used in the design of structural steel. The mentioned code did not consider the concrete confinement contribution to the axial capacity of concrete-filled tubes. It did not consider the triaxial loading condition, which clearly stated that the concrete compressive strength was increased. In the case of plastic stress distribution, AISC simply stated that the yield stress of the tube was

reached at 0.95  $fc'$ . The ultimate axial strength ( $P_{AISC}$ ) of CFDST columns was determined using Equation (3), as specified by AISC specification [57].

$$P_{AISC} = \begin{cases} P_{no} \left[ 0.658 \frac{P_{no}}{P_e} \right] & : \frac{P_{no}}{P_e} \leq 2.25 \\ 0.877 P_e & : \frac{P_{no}}{P_e} > 2.25 \end{cases} \quad (3)$$

where

$$P_e = \pi^2 \frac{(EI)_e}{(KL)^2}$$

where  $A_i$ ,  $A_o$  and  $A_c$  are the cross-sectional areas of the outer tube, inner tube, and infilled concrete, respectively.

According to AISC design rules, for all CFDST samples with inner steel tubes, the mean, standard deviation, and coefficient of variation (COV) were 1.29, 0.07, and 0.08, respectively. However, for samples with inner PVC tubes, these values were measured as 1.21, 0.07, and 0.09, respectively.

### 3.7.2. Han's Equation

Experimental results of CFDST columns were compared with the axial strength proposed by HAN et al. [58] for short square CFDST columns with an inner CHS. The predicted design strength ( $P_{HAN}$ ) was given by Equation (4). This equation was based on regression and did not consider the effect of outer tube geometry.

$$P_{HAN} = P_{osc,u} + P_{i,u} \quad (4)$$

where  $P_{i,u} = A_{si} \cdot f_{yi}$  is the compressive capacity of the inner tube, while  $P_{osc,u}$  is the combined capacity of the outer tube and infilled concrete.  $P_{osc,u}$  could be determined by  $f_{scy}$ .  $A_{osc}$  with  $A_{osc} = A_{os} + A_c$ , in which  $A_{os}$  and  $A_c$  was cross-sectional areas of the outer tube and infilled concrete. The strength  $f_{scy}$  was given by Equation (5):

$$f_{scy} = \left[ 1.212 + \left\{ 0.138 \frac{f_{yo}}{235} + 0.7646 \right\} \zeta + \left\{ -0.0727 \frac{f_c}{20} + 0.0216 \right\} \zeta^2 \right] f \quad (5)$$

where

$$f_c = 0.67 f'_c$$

and

$$\zeta = \frac{A_{so} \cdot f_{yo}}{A_c \cdot f_c}$$

According to the GB code, for all CFDST samples with inner steel tubes, the mean, standard deviation, and coefficient of variation (COV) were found to be 1.36, 0.11, and 0.09, respectively. However, for samples with inner PVC tubes, these values were measured as 1.11, 0.07, and 0.08.

### 3.7.3. Euro Code 4

Dissimilar to an AISC, in Euro Code 4, the buckling curves for the steel section were used without considering the element imperfection. According to EC4 [59], the design strength of CFDST columns was predicted by Equation (6) given below:

$$P_{EC4} = \chi \cdot P_u \quad (6)$$

where

$$P_u = f_{yo} \cdot A_{so} + f'_c \cdot A_c + f_{yi} \cdot A_{si}$$

The critical buckling load was determined using  $P_c = \pi^2 (EI)_e / (KL)^2$ , where  $KL$  is the effective length of the member. It should be noted that in the calculations, the effective

length was taken to be the actual length. The reduction factor ( $\chi$ ) used in Equation (3) was given in Equation (7):

$$\chi = \frac{1}{\left(\varnothing + \sqrt{\left(\varnothing^2 + \check{y}^2\right)}\right)} \leq 1.0 \text{ with } \varnothing = 0.5\left(1 + \alpha(\check{y} - 2) + \check{y}^2\right) \quad (7)$$

where  $\check{y} = \sqrt{(Pu/Pc)}$ , and  $\alpha$  can be determined from the buckling curve against the steel ratio ( $\rho_s$ ). The steel ratio of all the specimens used in this research laid within the range of 5 to 9%.

According to EC4 design rules, for all CFDST samples with inner steel tubes, the mean, standard deviation, and coefficient of variation (COV) were 1.36, 0.07, and 0.09, respectively. However, for samples with inner PVC tubes, these values were measured as 1.29, 0.07, and 0.09.

### 3.7.4. Comparison of Axial Capacity

The aforementioned equations lacked the clear description of the CFDSTs and CFSPTs, and had certain limitations. In order to check the accurateness and applicability of the design equation, it was necessary to analyze the experimental results against the predicted results of the described equations. Figure 8 presents the comparison between the experimental and predicted ultimate axial capacity of CFDST and CFSPT columns. It can be observed that all prediction equations over predicted the strength of CFDST columns with slender outer sections. Figure 8 shows that the AISC equation predicted more accurate results for CFDST columns, while Han's equation prediction accuracy stood well for CFSPT columns. Overall, Han's model showed the best results. The Eurocode gave higher error values for both CFDSTs and CFSPTs, which might have been due to the Eurocode's element imperfection factor.

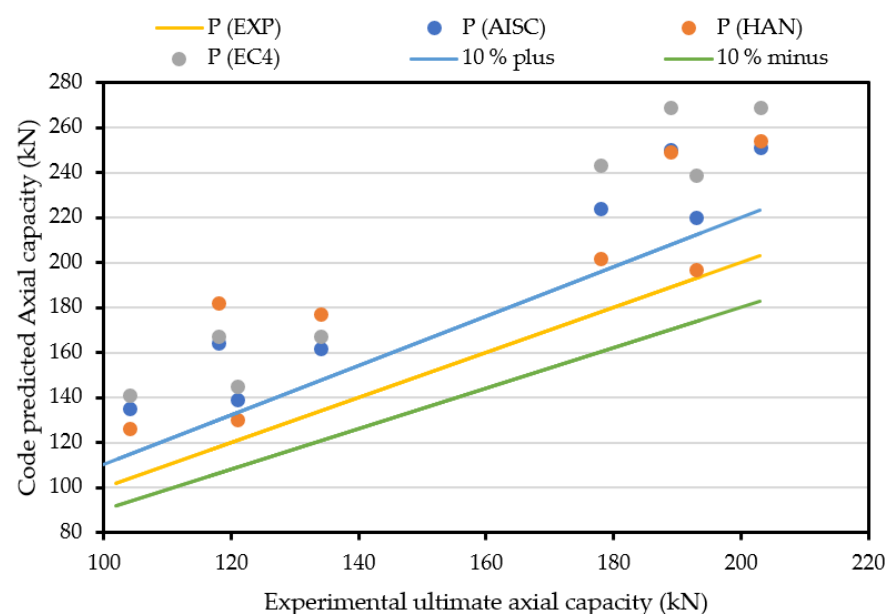


Figure 8. The normalized axial capacity of CFDST columns incorporating steel tube and PVC pipe.

## 4. Conclusions and Recommendations

This paper analyzed the use of PVC pipes in place of the inner steel tube in CFDSTs. Experimental investigations were carried out to study the effect of different parameters on the compression behavior of square CFDST columns. Moreover, the results obtained through experiments were compared with design equations presented by AISC, Han, and the Eurocode. The predicted strengths were found to be in good agreement with

the experimental results. The parameters considered were the outer tube slenderness, outer-to-inner tube dimension ratio, and type of inner tube. Results obtained through experimental investigation came to the following conclusions.

1. Almost a similar reduction in the axial load capacity of CFDST and CFSPT columns was noted with a similar reduction in the outer tube width to the outer tube thickness ratio ( $B_o/t$ ). The average strength of CFDSTs and CFSPTs was reduced by 42% and 47%, respectively, with the reduction in  $B_o/t$  by 25%.
2. Generally, the increasing trend in the strength of CFDST columns was observed with an increase in the outer-to-inner tube dimension ratio. This increase may have been due to the availability of a smaller area for the proper placement and compaction of infilled concrete.
3. No significant variation occurred in the ultimate axial capacity of CFDST columns with the inner PVC pipe compared to the steel inner tube. With the replacement of the inner tube of steel with a PVC pipe, on average, less than 10% strength was reduced, irrespective of the size and dimensions of the steel tube.
4. No eminent variation in the strength index and concrete contribution ratio was observed with the inner PVC pipe compared to the steel inner tube. For both groups of samples (CFDSTs and CFSPTs), the strength index was lesser than 1.
5. The capacity of CFDST columns with an inner steel tube was well predicted by the AISC strength equation, while the estimation of strength by Han's equation showed more accurate results for CFSPTs.

Only limited research was conducted on CFDST columns containing PVC as an inner tube. It is further recommended to study the influence of the slenderness, inner-to-outer dimension ratio, and exposure to fire on the strength of CFDSTs.

**Author Contributions:** Supervision, review, and editing, H.R. & M.F.J.; data curation and methodology, M.F.J.; investigation and review, M.A.K. and M.F.J.; conceptualization, data analysis, writing original draft preparation, M.F.J.; formal analysis and modeling, F.A.; validation, proofreading, review, M.A.M. and N.I.V. All authors have read and agreed to the published version of the manuscript.

**Funding:** The research was partially funded by the Ministry of Science and Higher Education of the Russian Federation as part of the World-class Research Center program: Advanced Digital Technologies (contract no. 075-15-2020-934 dated 17 November 2020).

**Data Availability Statement:** The data used in this research was collected from our own experimental work.

**Conflicts of Interest:** The authors declare no conflict of interest.

## References

1. Chen, C.C.; Chen, C.C.; Shen, J.H. Effects of steel-to-member depth ratio and axial load on flexural ductility of concrete-encased steel composite columns. *Eng. Struct.* **2018**, *155*, 157–166. [[CrossRef](#)]
2. Rehman, S.K.U.; Ibrahim, Z.; Memon, S.A.; Jameel, M. Nondestructive test methods for concrete bridges: A review. *Constr. Build. Mater.* **2016**, *107*, 58–86. [[CrossRef](#)]
3. Baghi, H.; Menkulasi, F.; Parker, J.; Barros, J.A.O. Development of a High-Performance Concrete Deck for Louisiana's Movable Bridges: Numerical Study. *J. Bridg. Eng.* **2017**, *22*, 04017028. [[CrossRef](#)]
4. Javed, M.F.; Hafizah, N.; Memon, S.A.; Jameel, M.; Aslam, M. Recent research on cold-formed steel beams and columns subjected to elevated temperature: A review. *Constr. Build. Mater.* **2017**, *144*, 686–701. [[CrossRef](#)]
5. Imran, M.; Mahendran, M.; Keerthan, P. Mechanical properties of cold-formed steel tubular sections at elevated temperatures. *J. Constr. Steel Res.* **2018**, *143*, 131–147. [[CrossRef](#)]
6. Abramski, M.; Korzeniowski, P.; Klempka, K. Experimental Studies of Concrete-Filled Composite Tubes under Axial Short- and Long-Term Loads. *Materials* **2020**, *13*, 2080. [[CrossRef](#)]
7. Chen, Z.; Tang, J.; Zhou, X.; Zhou, J.; Chen, J. Interfacial Bond Behavior of High Strength Concrete Filled Steel Tube after Exposure to Elevated Temperatures and Cooled by Fire Hydrant. *Materials* **2019**, *13*, 150. [[CrossRef](#)]
8. Ding, F.; Liao, C.; Wang, E.; Lyu, F.; Xu, Y.; Liu, Y.; Feng, Y.; Shang, Z. Numerical Investigation of the Composite Action of Axially Compressed Concrete-Filled Circular Aluminum Alloy Tubular Stub Columns. *Materials* **2021**, *14*, 2435. [[CrossRef](#)]
9. Krishan, A.; Rimshin, V.; Troshkina, E. Experimental research of the strength of compressed concrete filled steel tube elements. In *International Scientific Siberian Transport Forum*; Springer: Cham, Switzerland, 2020; pp. 560–566.

10. Krishan, A.L.; I Rimshin, V.; A Troshkina, E. Deformability of Volume-Compressed Concrete Core of Concrete Filled Steel Tube Columns. *IOP Conf. Ser. Mater. Sci. Eng.* **2020**, *753*, 022053. [[CrossRef](#)]
11. Liu, L.; He, L.; Cheng, Z.; Wang, X.; Ma, Z.; Cheng, X. Interface Bonding Behavior of Concrete-Filled Steel Tube Blended with Circulating Fluidized Bed Bottom Ash. *Materials* **2021**, *14*, 1529. [[CrossRef](#)] [[PubMed](#)]
12. Liu, S.; Ding, X.; Li, X.; Liu, Y.; Zhao, S. Behavior of Rectangular-Sectional Steel Tubular Columns Filled with High-Strength Steel Fiber Reinforced Concrete Under Axial Compression. *Materials* **2019**, *12*, 2716. [[CrossRef](#)] [[PubMed](#)]
13. Liu, W.; Cao, W.; Zhang, J.; Wang, R.; Ren, L. Mechanical Behavior of Recycled Aggregate Concrete-Filled Steel Tubular Columns before and after Fire. *Materials* **2017**, *10*, 274. [[CrossRef](#)] [[PubMed](#)]
14. Lv, J.; Zhou, T.; Du, Q.; Li, K.; Jin, L. Research on the Bond Behavior of Preplaced Aggregate Concrete-Filled Steel Tube Columns. *Materials* **2020**, *13*, 300. [[CrossRef](#)]
15. Lyu, X.; Xu, Y.; Xu, Q.; Yu, Y. Axial Compression Performance of Square Thin Walled Concrete-Filled Steel Tube Stub Columns with Reinforcement Stiffener under Constant High-Temperature. *Materials* **2019**, *12*, 1098. [[CrossRef](#)] [[PubMed](#)]
16. Shen, Y.; Tu, Y. Flexural Strength Evaluation of Multi-Cell Composite T-Shaped Concrete-Filled Steel Tubular Beams. *Materials* **2021**, *14*, 2838. [[CrossRef](#)] [[PubMed](#)]
17. Zhang, F.; Xia, J.; Li, G.; Guo, Z.; Chang, H.; Wang, K. Degradation of Axial Ultimate Load-Bearing Capacity of Circular Thin-Walled Concrete-Filled Steel Tubular Stub Columns after Corrosion. *Materials* **2020**, *13*, 795. [[CrossRef](#)] [[PubMed](#)]
18. Alatshan, F.; Osman, S.A.; Mashiri, F.; Hamid, R. Explicit Simulation of Circular CFST Stub Columns with External Steel Confinement under Axial Compression. *Materials* **2019**, *13*, 23. [[CrossRef](#)] [[PubMed](#)]
19. Al-Nini, A.; Nikbakht, E.; Syamsir, A.; Shafiq, N.; Mohammed, B.S.; Al-Fakih, A.; Al-Nini, W.; Amran, Y.H.M. Flexural Behavior of Double-Skin Steel Tube Beams Filled with Fiber-Reinforced Cementitious Composite and Strengthened with CFRP Sheets. *Materials* **2020**, *13*, 3064. [[CrossRef](#)] [[PubMed](#)]
20. Wang, Y.-H.; Lu, G.-B.; Zhou, X.-H. Experimental study of the cyclic behavior of concrete-filled double skin steel tube columns subjected to pure torsion. *Thin-Walled Struct.* **2018**, *122*, 425–438. [[CrossRef](#)]
21. Pagoulatou, M.; Sheehan, T.; Dai, X.; Lam, D. Finite element analysis on the capacity of circular concrete-filled double-skin steel tubular (CFDST) stub columns. *Eng. Struct.* **2014**, *72*, 102–112. [[CrossRef](#)]
22. Li, W.; Han, L.-H.; Chan, T.-M. Tensile behaviour of concrete-filled double-skin steel tubular members. *J. Constr. Steel Res.* **2014**, *99*, 35–46. [[CrossRef](#)]
23. Huang, H.; Han, L.-H.; Tao, Z.; Zhao, X.-L. Analytical behaviour of concrete-filled double skin steel tubular (CFDST) stub columns. *J. Constr. Steel Res.* **2010**, *66*, 542–555. [[CrossRef](#)]
24. Han, L.-H.; Huang, H.; Zhao, X.-L. Analytical behaviour of concrete-filled double skin steel tubular (CFDST) beam-columns under cyclic loading. *Thin-Walled Struct.* **2009**, *47*, 668–680. [[CrossRef](#)]
25. Uenaka, K.; Kitoh, H.; Sonoda, K. Concrete filled double skin circular stub columns under compression. *Thin-Walled Struct.* **2010**, *48*, 19–24. [[CrossRef](#)]
26. Lu, H.; Han, L.-H.; Zhao, X.-L. Fire performance of self-consolidating concrete filled double skin steel tubular columns: Experiments. *Fire Saf. J.* **2010**, *45*, 106–115. [[CrossRef](#)]
27. Wang, F.-C.; Han, L.-H.; Li, W. Analytical behavior of CFDST stub columns with external stainless steel tubes under axial compression. *Thin-Walled Struct.* **2018**, *127*, 756–768. [[CrossRef](#)]
28. Zhao, X.-L.; Grzebieta, R. Strength and ductility of concrete filled double skin (SHS inner and SHS outer) tubes. *Thin-Walled Struct.* **2002**, *40*, 199–213. [[CrossRef](#)]
29. Tao, Z.; Han, L.-H.; Zhao, X.-L. Behaviour of concrete-filled double skin (CHS inner and CHS outer) steel tubular stub columns and beam-columns. *J. Constr. Steel Res.* **2004**, *60*, 1129–1158. [[CrossRef](#)]
30. Tao, Z.; Han, L.-H. Behaviour of concrete-filled double skin rectangular steel tubular beam-columns. *J. Constr. Steel Res.* **2006**, *62*, 631–646. [[CrossRef](#)]
31. Li, W.; Ren, Q.-X.; Han, L.-H.; Zhao, X.-L. Behaviour of tapered concrete-filled double skin steel tubular (CFDST) stub columns. *Thin-Walled Struct.* **2012**, *57*, 37–48. [[CrossRef](#)]
32. Li, W.; Han, L.-H.; Ren, Q.-X.; Zhao, X.-L. Behavior and calculation of tapered CFDST columns under eccentric compression. *J. Constr. Steel Res.* **2013**, *83*, 127–136. [[CrossRef](#)]
33. Han, L.H.; Ren, Q.X.; Li, W. Tests on stub stainless steel—concrete—carbon steel double-skin tubular (DST) columns. *J. Constr. Steel Res.* **2011**, *67*, 437–452. [[CrossRef](#)]
34. Han, T.H.; Stallings, J.M.; Kang, Y.J. Nonlinear concrete model for double-skinned composite tubular columns. *Constr. Build. Mater.* **2010**, *24*, 2542–2553. [[CrossRef](#)]
35. Farajpourbonab, E.; Ebrahim, F. Effective parameters on the behavior of CFDST columns. *J. Appl. Eng. Sci.* **2017**, *15*, 99–108. [[CrossRef](#)]
36. Dong, C.; Ho, J. Concrete-filled double-skin tubular columns with external steel rings. In Proceedings of the Australian Earthquake Engineering Society 2012 Conference, Gold Coast, Australia, 7–9 December 2012.
37. Haas, T.N.; Koen, A. Eccentric loading of CFDST columns. *Int. J. Civ. Environ. Struct. Constr. Archit. Eng.* **2014**, *8*, 1262–1266.
38. Romero, M.L.; Espinós, A.; Portolés, J.; Hospitaler, A.; Ibáñez, C. Slender double-tube ultra-high strength concrete-filled tubular columns under ambient temperature and fire. *Eng. Struct.* **2015**, *99*, 536–545. [[CrossRef](#)]

39. Han, L.-H.; Tao, Z.; Huang, H.; Zhao, X.-L. Concrete-filled double skin (SHS outer and CHS inner) steel tubular beam-columns. *Thin-Walled Struct.* **2004**, *42*, 1329–1355. [[CrossRef](#)]
40. Elchalakani, M.; Zhao, X.-L.; Grzebieta, R. Tests on concrete filled double-skin (CHS outer and SHS inner) composite short columns under axial compression. *Thin-Walled Struct.* **2002**, *40*, 415–441. [[CrossRef](#)]
41. Yang, J.; Xu, H.; Peng, G. Behavior of concrete-filled double skin steel tubular columns with octagon section under axial compression. *Front. Arch. Civ. Eng. China* **2008**, *2*, 205–210. [[CrossRef](#)]
42. Wang, J.; Li, B.; Wang, D.; Zhao, C. Cyclic testing of steel beam blind bolted to CFST column composite frames with SBTD concrete slabs. *Eng. Struct.* **2017**, *148*, 293–311. [[CrossRef](#)]
43. Rashid, K.; Yazdanbakhsh, A.; Rehman, M.-U. Sustainable selection of the concrete incorporating recycled tire aggregate to be used as medium to low strength material. *J. Clean. Prod.* **2019**, *224*, 396–410. [[CrossRef](#)]
44. ASTM International Committee C09 on Concrete and Concrete Aggregates. *Standard Test Method for Compressive Strength of Cylindrical Concrete Specimens*; ASTM International: West Conshohocken, PA, USA, 2001.
45. ASTM, E. 8M: Standard test methods for tension testing of metallic materials (Metric). In *Annual Book of ASTM Standards*; ASTM International: West Conshohocken, PA, USA, 2003; Volume 3.
46. Romero, M.L.; Ibáñez, C.; Espinós, A.; Portolés, J.; Hospitaler, A. Influence of Ultra-high Strength Concrete on Circular Concrete-filled Dual Steel Columns. *Struct.* **2017**, *9*, 13–20. [[CrossRef](#)]
47. Wang, Z.-B.; Tao, Z.; Yu, Q. Axial compressive behaviour of concrete-filled double-tube stub columns with stiffeners. *Thin-Walled Struct.* **2017**, *120*, 91–104. [[CrossRef](#)]
48. Hassanein, M.; Kharoob, O.; Liang, Q. Circular concrete-filled double skin tubular short columns with external stainless steel tubes under axial compression. *Thin-Walled Struct.* **2013**, *73*, 252–263. [[CrossRef](#)]
49. Hassanein, M.; Kharoob, O. Analysis of circular concrete-filled double skin tubular slender columns with external stainless steel tubes. *Thin-Walled Struct.* **2014**, *79*, 23–37. [[CrossRef](#)]
50. Ekmekyapar, T.; Al-Eliwi, B.J. Concrete filled double circular steel tube (CFDCST) stub columns. *Eng. Struct.* **2017**, *135*, 68–80. [[CrossRef](#)]
51. Teng, J.-G.; Wang, Z.; Yu, T.; Zhao, Y.; Li, L.-J. Double-tube concrete columns with a high-strength internal steel tube: Concept and behaviour under axial compression. *Adv. Struct. Eng.* **2018**, *21*, 1585–1594. [[CrossRef](#)]
52. Yuan, F.; Chen, M.; Huang, H.; Xie, L.; Wang, C. Circular concrete filled steel tubular (CFST) columns under cyclic load and acid rain attack: Test simulation. *Thin-Walled Struct.* **2018**, *122*, 90–101. [[CrossRef](#)]
53. Hassanein, M.; Patel, V. Round-ended rectangular concrete-filled steel tubular short columns: FE investigation under axial compression. *J. Constr. Steel Res.* **2018**, *140*, 222–236. [[CrossRef](#)]
54. Li, W.; Han, L.-H.; Zhao, X.-L. Axial strength of concrete-filled double skin steel tubular (CFDST) columns with preload on steel tubes. *Thin-Walled Struct.* **2012**, *56*, 9–20. [[CrossRef](#)]
55. Wang, W.-H.; Han, L.-H.; Li, W.; Jia, Y.-H. Behavior of concrete-filled steel tubular stub columns and beams using dune sand as part of fine aggregate. *Constr. Build. Mater.* **2014**, *51*, 352–363. [[CrossRef](#)]
56. Han, L.-H. Tests on stub columns of concrete-filled RHS sections. *J. Constr. Steel Res.* **2002**, *58*, 353–372. [[CrossRef](#)]
57. Leon, R.T.; Hajjar, J.F. Limit State Response of Composite Columns and Beam-Columns. Part II: Application of Design Provisions for 2005 AISC Specification. *Eng. J.* **2008**, *45*, 21–46.
58. Han, L.-H.; Tao, Z.; Liu, W. Concrete filled steel tubular structures from theory to practice. *J. Fuzhou Univ.* **2017**, *6*, 3.
59. Roik, K.; Bergmann, R. *EUROCODE 4: Composite Columns*; Report EC4/6; Ruhr-Universität Bochum: Bochum, Germany, 2005.